Natural hydraulic fracturing

Terry Engelder & Alfred Lacazette
The Pennsylvania State University, University Park, Pennsylvania 16802 USA

Engelder, T., and Lacazette, A., 1990, Natural Hydraulic Fracturing, in Barton, N., and Stephansson, O., eds., Rock Joints, A.A. Balkema, Rotterdam, p. 35-44.

ABSTRACT: The surface morphology of cross-fold joints in the Devonian Ithaca siltstone near Watkins Glen, New York, is used to constrain hypotheses concerning joint initiation under conditions of abnormally high fluid pressure. Joint initiation took place at 1 - 3 cm diameter flaws (i.e. fossils, concretions, flute casts). Assuming that in situ properties of the Ithaca siltstone match laboratory values (i.e. $K_{IC} = 2.5$ MPa $m^{1/2}$ and $\nu = 0.17$), the application of linear elastic fracture mechanics suggests that cross-fold joints in the siltstone were initiated from fossils, concretions, and flute casts when the pore pressure was about 85% of the overburden stress. At joint initiation pore pressure inside the flaw was the same as pore pressure in the matrix of the rock. The driving stress for joint initiation arises from the poroelastic behavior of the Ithaca siltstone. As the joint grows in volume through propagation, fluid pressure within the joint drops and propagation is arrested. Once the joints have grown to lengths greater than initial flaw size, crack propagation is reinitiated at internal fluid pressures that are less than pore pressure within the rock matrix. With relatively low reinitiation pressures a pressure gradient is created which will maintain flow from the matrix to the joint and, hence, continuously recharge fluid pressure within the joint.

1 INTRODUCTION

Secor's (1965; 1969) classic model for jointing under the influence of pore pressure recognizes three stages to joint growth: initiation, propagation and arrest. The model postulates that joints initiate from randomly oriented small cracks or flaws which are loaded internally by pore fluid within the rock mass. Joint initiation may occur once fluid within the crack acts outward against compressive rock stress with enough force to subject the crack to a net tensile stress. This form of fluid-induced joint growth is akin to fracture propagation during oil well hydraulic fracturing (OWHF) and here is called natural hydraulic fracturing (NHF) (Secor, 1965; Beach, 1977; Engelder, 1985). Rules for joint propagation in Secor's model closely follow Griffith's energy balance approach which was recently reviewed by Lawn and Wilshaw (1975) and Broek (1987). The net tensile stress arising from internal fluid pressure is the driving stress for joint propagation. Secor's model states that joint propagation will arrest once the driving stress is relieved by drop in fluid pressure which accompanies growth of crack volume. According to the model joint growth by NHF takes place in increments and not during one continuous rupture as in an OWHF. Secor's model was in part based on the morphology of crack-seal veins, millifractures, and joints.

Price (in Fyfe et al, 1978) and more recently Gretener (1981) have correctly pointed out that Secor's model neglects the role of pore pressure (i.e. poroelasticity) in increasing the total stress on the crack wall. Although Fyfe et al (1978) appear to recognize that Secor's (1965) mechanism is viable if the general law of effective stress (Nur and Byerlee, 1971) is used in place of the simple law, their analysis can be clarified. In this paper we show that fracture initiation and propagation by NHF is theoretically possible according to the general law of effective stress where the crack driving stress arises from the poroelastic behavior of the rock. We define some of the conditions which favor NHF in sedimentary basins. For field evidence we draw upon the surface morphology seen on cross-fold joints cutting the Ithaca siltstone, a formation in the Devonian Catskill Delta of the Appalachian Basin, New York (Figure 1).

2 THE EFFECT OF POROELASTICITY

The poroelastic effect may be visualized using a force-balance model (Figure 2). This rock model contains grains elastic grain-grain contacts and pore space between the grains. All the pores are interconnected so that the aggregate has some finite permeability. An initial flaw or small crack is introduced into the aggregate of grains and elastic grain-grain contacts by a cut through the center of the model. Two halves of the aggregate are compressed together in a container with rigid walls. Initially the aggregate is dry so that the rigid walls of the container press the initial flaw together with an average force per unit area, S_t. S_t represents a rock stress normal to the flaw. The aggregate is then filled with a pore fluid at a relatively low pressure of P_p. If the face of the initial flaw is considered as an impermeable interface, the additional of pore fluid would not cause a uniform increase in stress along the interface. Where pore fluid was in direct contact with the interface the pressure on the interface would increase by P_p. Where grains were in contact with the interface the normal stress on the interface would increase by a fraction, α, of P_p. This fractional increase in normal stress arises because the grains are connected by elastic contacts which take-up part of the force exerted by pore fluid inside pores. This partial transfer of pore pressure to the aggregate boundary is known as the poroelastic effect (Biot, 1941). Any increase in P_p along the initial flaw will act to open the initial flaw but this increase is partially counterbalanced by a poroelastic expansion of the aggregate which acts to keep the initial flaw closed.

To initiate crack propagation for both OWHF and NHF, internal fluid pressure must counterbalance the total least principal stress, σ_3 (i.e. $S_t + \alpha P_p$ in the model shown in Figure 2). Because we deal with vertical joints in this paper, we set the total least horizontal stress, S_h, equal to σ_3. In saturated rocks total stress may be divided into two components: the stress carried by grain-grain contacts under dry conditions (i.e. S_t in Figure 2) and stress generated by fluid pressure within pore space of the rock (i.e. αP_p in Figure 2). By the poroelastic effect an increase in P_p will cause an increase in total stress provided that the rock is constrained by rigid boundaries. One type of rigid boundary behavior is called uniaxial strain which is a common model for horizontal strain in sedimentary basins (Geertsma, 1957):

$$\varepsilon_H = \varepsilon_h = 0 \tag{1a}$$

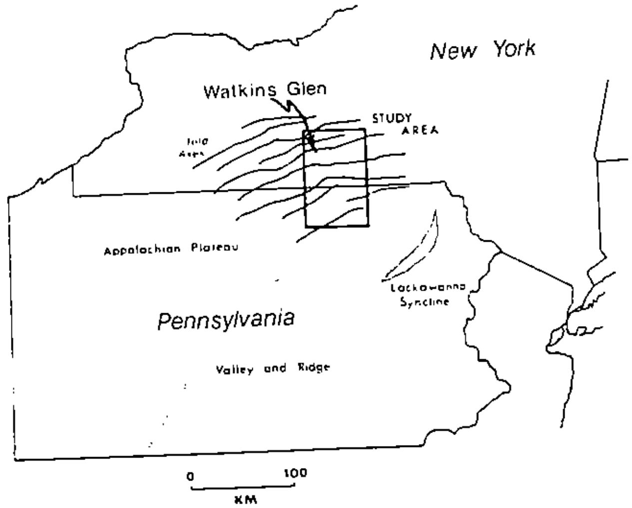

Figure 1. Field examples of NHF come from an outcrop on the south side of Watkins Glen, New York. This outcrop has been described in Bahat and Engelder (1984) and Engelder et al (1987).

$$\varepsilon_v \neq 0 \tag{1b}$$

ε_H and ε_h are principal strains in the horizontal direction. The effect of a change in pore pressure in sedimentary basins may be seen by solving Biot's (1941) elasticity equations for uniaxial strain. Biot's elasticity equations are given by Rice and Cleary (1976) as

$$2\Gamma\varepsilon_{ij} = \langle\sigma_{ij}\rangle - \frac{\nu}{1+\nu}\langle\sigma_{kk}\rangle\delta_{ij} \tag{2a}$$

where

$$\langle\sigma_{ij}\rangle = \sigma_{ij} + \alpha P_p \tag{2b}$$

In Biot's equations α is Biot's poroelastic term defined as $\{1 - C_i/C_b\}$ with the intrinsic compressibility of the uncracked solid, C_i (i.e. the compressibility of the solid grains in Figure 2), and the bulk compressibility of the solid with cracks and pores, C_b (i.e. the compressibility controlled largely by the aggregate in Figure 2) (Nur and Byerlee, 1971). Γ and ν are the shear modulus and Poisson ratio of the rock when it is deformed under 'drained' conditions.

For our analysis of vertical joints and veins, the crack-normal stress would have been the least horizontal stress, S_h. Little is known about the least horizontal stress in a sedimentary basin where vertical joints are forming except the obvious; the

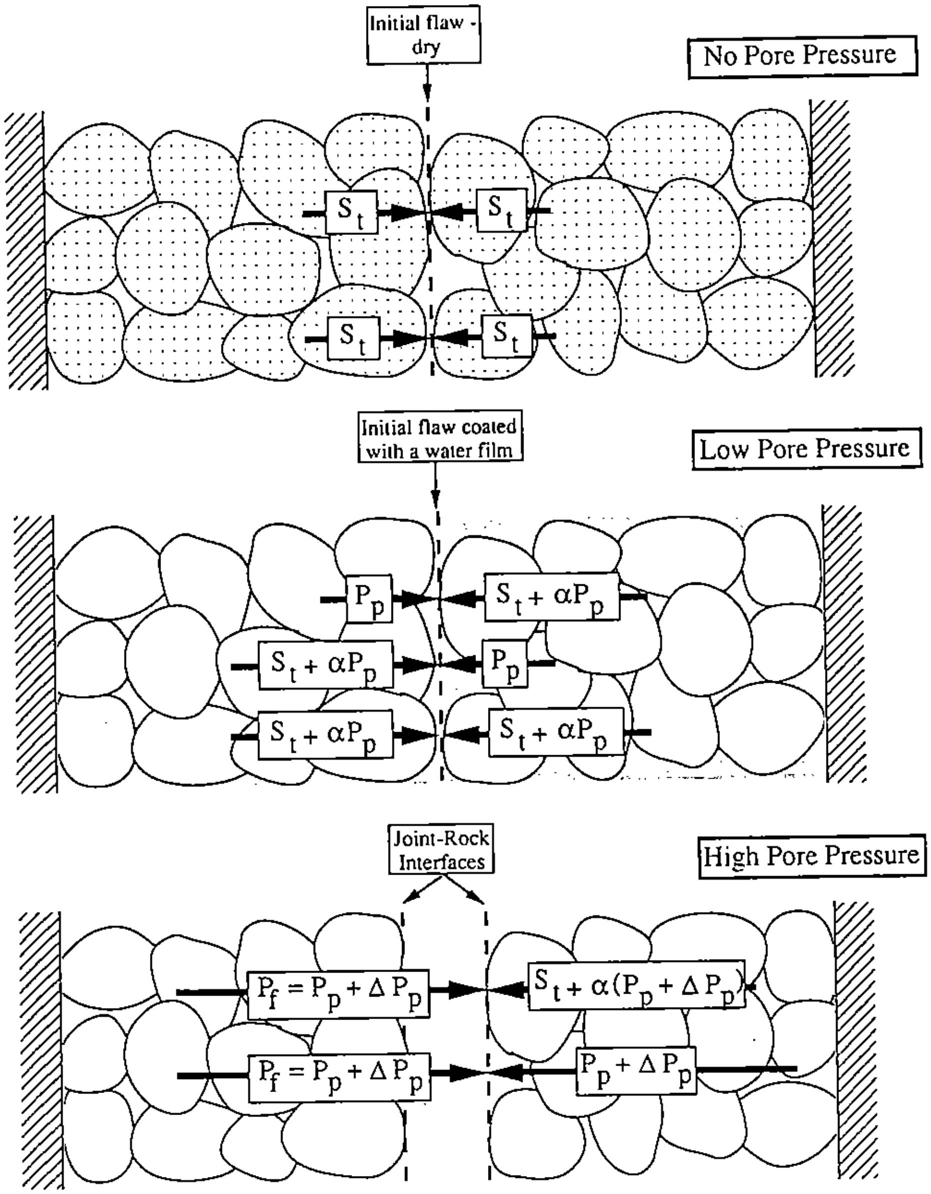

Figure 2. Poroelastic model for a rock with an initial flaw and constrained by rigid boundaries on all sides. The model consists of grains, elastic grain-grain contacts, and interconnected pore space. Vectors are shown to represent the balance of forces along the interface between the initial flaw and the joint-rock surface.

total horizontal stress, $S_h < S_v$. The total vertical stress is

$$S_v = \rho_t g z \tag{3}$$

where ρ_t is the integrated density of the rock to the depth, z, of interest and g is the acceleration of gravity. Although the state of stress was probably more complicated in the case we will examine, we make the simplifying assumption that S_h was equal to that found in a tectonically relaxed basin. We define a tectonically relaxed basin as one in which S_h was proportional to S_v through the uniaxial elastic strain model:

$$S_h = \frac{\nu}{1-\nu} S_v \tag{4}$$

Solving Biot's elasticity equations for uniaxial strain we derive

$$S_h = \frac{\nu}{1-\nu} S_v - \frac{(1-2\nu)}{(1-\nu)} \alpha P_p \tag{5a}$$

In this equation tension is positive. Terms in this equation may be rearranged to appear in the same form as equation (#13) derived by Anderson et al (1973) for fracture pressure at a borehole

$$S_h = \frac{\nu}{1-\nu}(S_v - \alpha P_p) + \alpha P_p \tag{5b}$$

The two terms on the right-hand side of equation 5a are equivalent to but not the same as S_t and αP_p, respectively in Figure 2.

The internal fluid pressure, P_i, necessary to initiate crack propagation and thereby cause NHF is a function of several general parameters including total rock stress normal to the crack plane, S_h, and the elastic properties of the rock. To understand the variation of P_i, it is appropriate to consider the variation of S_h due to the poroelastic effect in a tectonically relaxed basin (Figure 3). The calculations for Figure 3 assume 3 km of overburden which is about the depth at which cross-fold joints propagated in the Ithaca siltstone and the depth for the top of the abnormally high pore pressures in the Gulf of Mexico. Overburden is assumed to have a density of 2.7 g/cc so that S_v = 79.5 MPa. An α of 0.7 as measured for Ithaca siltstone is also assumed (Table 1). S_h can vary as much as 50% of the overburden weight depending on ν and P_p. A larger S_h is generated in rock with a higher ν. The field of interest in Figure 3 is defined by $P_p > S_h$ for it is within this field that NHF occurs. In rocks with a very low ν, conditions favoring NHF may be found even at hydrostatic pore pressure whereas for rocks with a high ν conditions for NHF is suppressed until much a higher P_p has been reached.

3 THE INITIATION OF NHF - THEORY AND AN EXAMPLE

Joint initiation may be introduced by pointing out two important differences between an OWHF and NHF. First, to a rough approximation an OWHF boosts the internal pressure of a borehole (i.e. the initial flaw) without an accompanying increase in pore pressure in the rock behind the borehole wall. There may be some infiltration through the mudcake on the wall of the borehole but infiltration is confined to the immediate vicinity of the borehole. Prior to the initiation of NHF internal pressure within the initial flaw increases at the same rate as pore pressure in the rock behind the wall of the flaw. For an OWHF a pore pressure increase would decrease breakdown pressure whereas for extension of a penny-shaped flaw during NHF an increase in pore pressure adds to the internal pressure necessary for crack initiation. Second, the crack driving stress for OWHF does not drop abruptly after crack initiation because the borehole is continually being charged from surface pumps. In contrast, crack driving stresses for NHF drop either immediately or soon after crack initiation (Secor, 1969). Both of these differences impact on our understanding of NHF.

The following are reasons for making the assumption that $P_i = P_p$ at the initiation of NHF. In sedimentary rocks, even with a very low permeability, fluid pressure in one pore will tend to equilibrate with pressure in surrounding pores provided that the pores are interconnected. Although

Table 1. Properties of the Ithaca siltstone

Property	Value	Orientation
Bulk Density	2.62 g/cc	
Young's Modulus	56 GPa	BN
Young's Modulus	73 GPa	BP
Intrinsic Compress.	1.3×10^{-11} Pa^{-1}	BP
Bulk Compressibility	4.8×10^{-11} Pa^{-1}	BP
Biot's Constant (α)	0.7	BP
Poisson's Ratio (ν)	0.17	BN
K_{IC} (c_c = 82 mm)	2.66 MPa$\cdot\sqrt{m}$	BN
K_{IC} (c_c = 11 mm)	1.74 MPa$\cdot\sqrt{m}$	BN
K_{IC} (c_c = 2 mm)	1.26 MPa$\cdot\sqrt{m}$	BN
K_{IC} (c_c = 80 mm)	2.02 MPa$\cdot\sqrt{m}$	BP
K_{IC} (c_c = 11 mm)	1.31 MPa$\cdot\sqrt{m}$	BP

Data from I. Meglis, A. Lacazette, Scott (1989), Evans et al. (1989)

BP - bedding parallel; BN - bedding normal

Measurement of n taken from a silty mudstone of the West River Formation

c_c - Critical crack length at the onset of rapid crack propagation

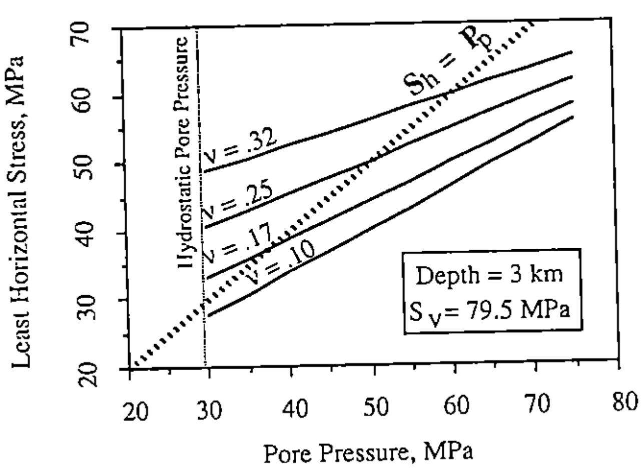

Figure 3. The relationship between S_h and P_p in a tectonically relaxed basin assuming poroelastic behavior. In a tectonically relaxed basin horizontal stresses are due solely to the overburden load. The poroelastic effect is strongly dependent on Poisson's ratio, ν, as indicated by the four curves for various values of ν. This calculation assumes conditions at a depth of burial of 3 km.

in some geologically relevant cases such as igneous dike intrusion it may be possible to have a fracture pressure in excess of pore pressure, in a typical sedimentary basin, there is no known mechanism for suddenly increasing pressure in one pore relative to its neighbors as is the case for an OWHF where $P_i > P_p$. As abnormally high pressures develop in sedimentary basins, pore pressure increases uniformly in the immediate vicinity of the incipient joint and so the mechanism for the initiation of NHF must operate even though $P_i = P_p$.

It is not intuitively obvious that a net tensile stress (i.e. a crack driving stress) can be generated along an initial flaw for several reasons: 1.) a compressive stress, S_h, increases as a function of P_p; 2.) pores of the rock behind the flaw are also subject to the same pressure; and 3.) fluids can readily drain from the flaw to the pore space. Furthermore, a possible analog to the joint-rock interface of Figure 2 is the face of an earth dam. Such an earth dam is stable because there is no net force against the face of the dam. However, there is a critical difference between soil in the earth dam and rock behind the joint-rock interface. Soil in the earth dam has an $\alpha = 1$ whereas for rock $\alpha < 1$.

The poroelastic behavior of rock, for which $\alpha < 1$, is responsible for the generation of a net tensile stress against the face of a flaw. Poroelastic behavior is illustrated using a force-balance model along the flaw-rock interface (Figure 2). Consider the effect of increasing pore pressure by an amount, ΔP_p. Fluid pressure in the flaw, P_f, is balanced by $P_p + \Delta P_p$ where pore space is against the interface. But by the poroelastic effect, the pore pressure increase does not cause normal stress to increase under a grain at the same rate. Hence, a condition will be reached in which P_f will exceed the normal stress exerted by grains on the interface. Once this condition is reached a net tensile force will act to compress the rock and, hence, push the joint-rock interfaces apart (Figure 2).

In addition to total rock stress, the internal fluid pressure, P_i, necessary to initiate joint propagation is a function of the fracture toughness of the rock, K_{IC}, the crack length, 2c, and the shape of the crack, Y. K_I, a measure of the stress concentration at a crack tip, increases with an increase in net tensile stress on the crack. K_{IC}, the critical stress intensity factor or fracture toughness is a material property that indicates the ease with which a rock will fracture. K_{IC} is a laboratory measure of the pull normal to a crack plane at the time the crack tip propagates rapidly. Joint initiation occurs only when the crack (i.e. initial flaw) walls are pulled apart or subject to a net tensile stress as a consequence of the poroelastic effect. The linear elastic fracture mechanics equation for the rapid growth of a joint is

$$P_i = \left\{ \frac{K_{IC}}{Yc^{\frac{1}{2}}} \right\} \tag{6a}$$

This is the condition in a dry rock if the walls of the crack are not supported by a remote earth stress. If the walls of the crack are forced closed by S_h and a pore fluid is present, then

$$P_i = \left\{ \frac{K_{IC}}{Yc^{\frac{1}{2}}} \right\} - \frac{\nu}{1-\nu} S_v + \frac{(1-2\nu)}{(1-\nu)} \alpha P_p \tag{6b}$$

P_p is positive where S_v is negative. As equation 6b indicates, P_i can vary significantly depending on the size of the pre-existing crack. In Figure 2 the difference between the length of the vector for normal stress across a grain and the vector for fluid pressure within the crack is the vector for $K_{IC}/Y_C{}^{1/2}$.

The equations developed above may be used in conjunction with measured rock properties to constrain the stress and pore pressure conditions under which a given set of natural hydraulic fractures initiated. Under the assumption that joints formed by NHF started propagating rapidly from small cracks or flaws when $P_i = P_p$, equation 6b may be rewritten to give an indication of flaw length leading to initiation of joints.

$$c = \left[\frac{K_{IC}}{Y\left\{ P_i + \frac{\nu}{1-\nu} S_v - \frac{(1-2\nu)}{(1-\nu)} \alpha P_p \right\}} \right]^2 \tag{7}$$

3.1 Initiation of NHF in the Ithaca siltstone

In this section we constrain conditions for the initiation of NHF assuming the properties of the Ithaca siltstone. Scott (1989) measured the fracture toughness of the Ithaca siltstone and found that it followed R-curve behavior (Broek, 1987) so that the K_{IC} decreases as of the size of the crack gets smaller. This suggests that a lower K_{IC} should be used for calculating crack initiation conditions than for calculations related to propagation of a joint once it has achieved dimensions of a meter of more. The lowest value of K_{IC} determined by Scott (1989) for the bedding perpendicular orientation in the Ithaca siltstone was 1.26 ± 0.06 MPa $m^{1/2}$ while the

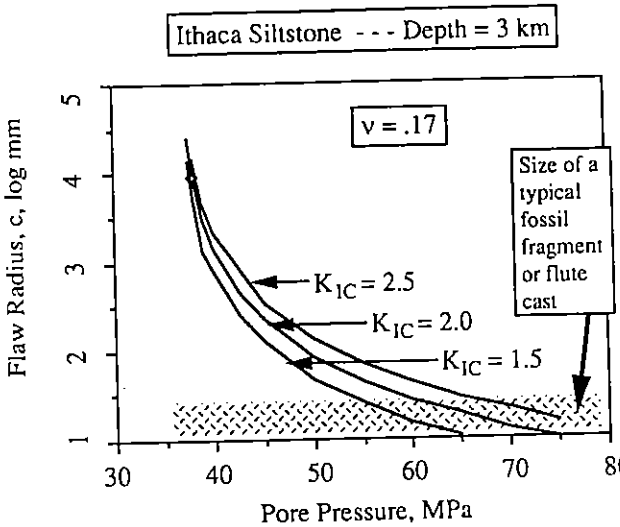

Figure 4. The relationship between flaw or crack length and pore pressure required to initiate cross-fold joint propagation in a tectonically relaxed basin assuming poroelastic behavior. The flaw length at initiation of propagation is moderately dependent on the K_{IC} of the rocks within which crack propagation takes place. This calculation assumes a penny-shaped flaw, a burial depth of 3 km and a ν of 0.17 for the Ithaca siltstone.

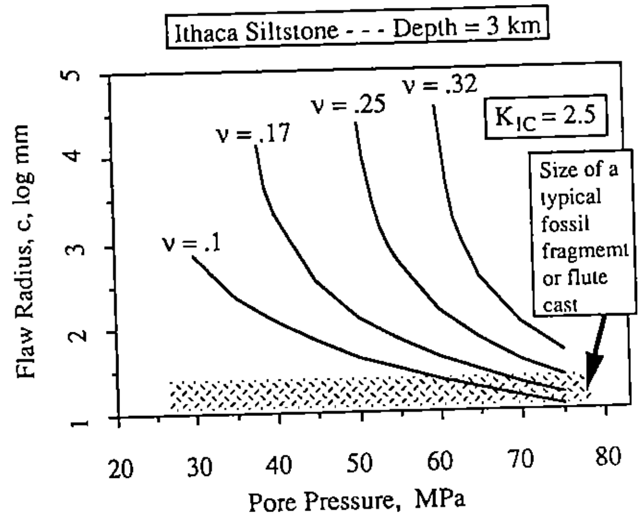

Figure 5. The relationship between flaw or crack length and pore pressure required to initiate crack propagation within the Ithaca siltstone. The flaw length at initiation of cross-fold joints is strongly dependent on the Poisson's ratio of the rocks within which crack propagation takes place. This calculation assumes a penny-shaped flaw, a tectonically relaxed basin with a poroelastic response to changes in pore pressure, a burial depth of 3 km, and a K_{IC} of 2.5 MPa-m$^{1/2}$ for the Ithaca siltstone.

highest value was 2.66 ± 0.07 MPa m$^{1/2}$. Typically K_{IC} of rocks varies between 2.5 MPa.m$^{1/2}$ and 1.5 MPa.m$^{1/2}$ (Atkinson, 1984). Laboratory measurements of ν for siltstones of the Appalachian Plateau suggests that $\nu = 0.17$ is reasonable for the Ithaca siltstone (Evans et al., 1989) (Table 1). All flaws in the Ithaca siltstone are assumed to be penny-shaped cracks which have Y = 1.13. Using equation 7 we calculate the flaw radius for fracture for NHF initiation within the Ithaca siltstone as a function of pore pressure at a depth of 3 km. These calculations assume three arbitrarily values of K_{IC} for joint initiation (2.5, 2.0, and 1.5 MPa m$^{1/2}$) (Figure 4). Figure 4 shows that joints will initiate from larger flaws at lower P_p.

At an early stage in their development rocks have no large joints but rather either microcracks in the form of pore space and grain boundaries or flaws in the form of fossil and/or rock fragments and sedimentary structures like flute casts at bedding boundaries. Unfractured Ithaca siltstone has two types of flaws: grain boundary microcracks and larger structures such as flute casts, concretions, and fossil fragments. Grain-boundary microcracks are on the scale of individual grains less than 0.1 mm in diameter. In contrast, fossil fragments and flute casts are roughly 1-3 cm in diameter. The plumose surface morphology on the surface of cross-fold joints in the Ithaca siltstone allows the joint propagation to be traced back to origin flaws which are commonly a 1-3 cm structures. From this observation we know the flaw size, 2c, for the initiation of NHF. Assuming conditions in a tectonically relaxed basin at a depth of 3 km, pore pressure at the initiation of NHF was on the order of 65 MPa or higher within the Ithaca Siltstone.

Figures 4 and 5 illustrate several points concerning the effect of both ν and K_{IC} on the flaw length for the initiation of joints within the Ithaca siltstone. First, grain boundary microcracks are too small to account for the initial propagation of NHF, even if siltstones of the Appalachian Plateau had an extremely low ν. Second, abnormal pore pressures, significantly above hydrostatic, were necessary for the initiation of joints at depth. Third, at $\nu = 0.17$, typical fossil fragments or flute casts were large enough flaws to favor the initiation of cross-fold joints at 3 km. Because we know this from outcrop evidence, we can calculate pore pressure at the initiation of joint propagation. Fourth, in a bedded siltstone-shale sequence, the initiation of NHF is favored in a rock with a lower ν (i.e. a siltstone) relative to a rock with higher ν (i.e. a shale).

3.2 Fluid pressure during joint propagation

Once joints have initiated from small flaws, less severe internal pressures are necessary for further growth. Equation 7 can also be used to calculate the incremental crack propagation pressure. Suppose that a cross-fold joint initiates from an initial flaw with a radius of about 1 cm. At initiation $P_p = P_i$ = 68 MPa (Figure 4). By the time the joint has run to a length of 30 cm, an internal pressure 20 MPa less than P_p is required for reinitiation of joint propagation. Figure 6 illustrates the difference between crack initiation pressure and crack propagation pressure. Crack initiation pressure is indicated by the dashed line cutting across the propagation pressure-pore pressure lines for joints of various lengths. Once a joint propagates to a length of more than one m, the crack propagation pressure changes very little. However, that pressure may be 20 MPa less than the crack initiation pressure.

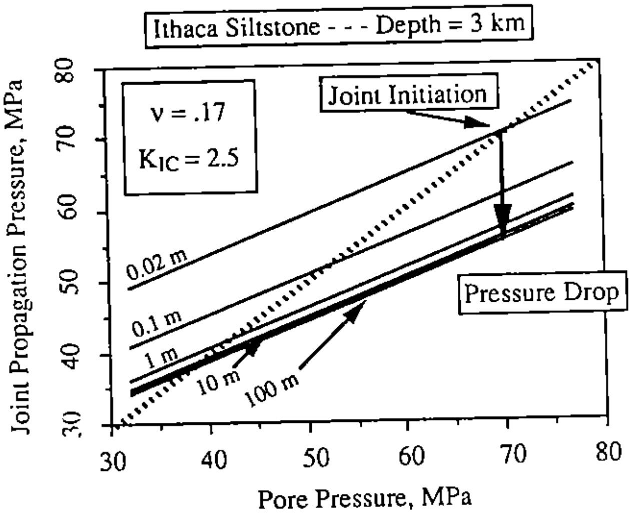

Figure 6. The relationship between crack propagation pressure and pore pressure for cross-fold joint of lengths between 0.02 m and 100 m. This calculation assumes a tunnel crack, a burial depth of 3 km, a K_{IC} of 2.5 MPa-m$^{1/2}$, and a ν of 0.17 for the Ithaca siltstone.

4 DISCUSSION

4.1 Alternative mechanisms for joint initiation on the Appalachian Plateau

We hypothesize that the cross-fold joints in the Ithaca siltstone at Watkins Glen were produced by NHF. The above calculations only show that this hypothesis is mechanically admissible even though $P_i = P_p$. Other mechanisms for joint initiation must be considered before this hypothesis can be accepted. Hydraulic fracturing by injection of pressurized fluid from an external source, axial splitting, and fracturing by true rather than effective tension must be considered as possible mechanisms.

The cross-fold joint set was the first to form (Bahat and Engelder, 1984) so that these joints formed in isolation and, therefore, could not have been connected to an external reservoir of high pressure fluid. Fracturing by true rather than effective tension may be ruled out largely because earth stress measurements show that true tension is not found on a mesoscopic scale within the crust.

Compression-parallel tension fractures may propagate unstably when a rock is compressed under even very slight lateral tension. This phenomena, known as axial splitting, is reviewed and analyzed by Horii and Nemat-Nasser (1985). Axial splitting results from the formation of a tensile zone at the tip of a discontinuity that has been activated in shear under the influence of the resolved shear stress. If a substantial confining pressure is present, then crack growth is stable and any increase in crack length must result from bulk shortening of the sample. Fractures formed by axial splitting should have a characteristic hook shaped geometry near the origin flaw (see Figures 2-4,6,8-10 of Horii and Nemat-Nasser, 1985), while the origin flaw itself should be a planar discontinuity at an angle to the fracture surface and should show evidence of shear deformation. Observations of the joint surface morphology near the initiation point show that these joints did not form by axial splitting. (Figure 6b in Bahat and Engelder, 1984). The delicate surface morphology allows the joint to be traced back to the origin flaw which shows no sign of shearing. The joint surface is highly planar both near to and away from the flaw. This shows that the joints initiated and propagated as pure opening mode fractures and were never subjected to a shear component even at the scale of the origin flaw. Another argument against axial splitting is the requirement of slight lateral tension for unstable crack propagation by this mechanism. We have already argued that substantial confining pressure must have been present at the time of joint formation. It is therefore unlikely that the observed joints, which are at least 3 orders of magnitude longer than their origin flaws, could have been generated by this mechanism.

We conclude that in-situ NHF as described above is the most likely mechanism to have produced cross-fold joints. Although our paper to this point implies that cross-fold joints on the Appalachian Plateau propagated under the influence of abnormally high pore pressures, the possibility exists that such joints could have initiated under conditions of hydrostatic pore pressure. Calculations show that effective tension under conditions of hydrostatic pore pressure develops only if S_h becomes considerably less than is found for a tectonically relaxed basin. Such conditions may be found in an actively slumping basin margin such as the northern Gulf of Mexico or during uplift and erosion under plane strain conditions (Voight and St. Pierre, 1974; Narr and Currie, 1982). However, our bias still is that the strong affinity between cross-fold joints and other Alleghanian structures (e.g. Engelder and Geiser, 1980; Engelder, 1985; Engelder and Oertel, 1985; Evans et al, 1989) suggests that abnormally high pore pressures were responsible for NHF on the Appalachian Plateau.

Regardless, the term NHF should not be restricted to those situations where joints propagate under abnormally high pore pressures. Rules such as poroelastic behavior which apply to joint initiation operate independently of the absolute magnitude of the pore pressure.

4.2 The Appalachian Basin as a tectonically relaxed basin

The assumption that S_h was close to conditions found in a tectonically relaxed basin can be evaluated with Figure 3. If S_h consisted of a tectonic component of as little 10 MPa above that for a relaxed basin, an additional 10 MPa of internal fluid pressure would have been required to initiate crack growth. That additional 10 MPa would have favored the lifting of overburden and the propagation of bedding parallel joints. In fact, the propagation of bedding-parallel joints is favored in the early stages of fold-thrust development prior to relaxation of the least horizontal stress (Lacazette and Engelder, 1987).

If earth stress in all directions were equal under conditions of hydrostatic pore pressure, the increase in pore pressure to fracture initiation would favor the propagation of horizontal cracks. This is an effect of the uniaxial strain model where stress due to poroelastic effect meets no resistance in the vertical direction. The vertical direction expands to relieve any increase in stress above overburden weight. However, an increase in stress due to the poroelastic stress is met with the resistance of fixed boundaries in the horizontal directions. As a consequence of this situation the S_h becomes larger than S_v as crack propagation conditions are approached. K_{IC} for Ithaca siltstones of the Appalachian Plateau is anisotropic with the vertical cross-fold direction having a higher 25% K_{IC} than horizontal cross-fold direction (Table 1). Thus, the anisotropy in K_{IC} of the Ithaca siltstone further favors horizontal crack propagation by about 5 MPa. To compensate for this anisotropy and favor vertical crack initiation, S_h prior to the buildup of pore pressure must have started out 5 MPa lower than would have been the case for an isotropic rock. According to Figure 4 S_h must have been within 5 MPa of relaxed conditions to favor vertical crack propagation.

4.3 Effect of variation in lithology

The Ithaca Formation also contains a fine example of the role which variation in lithology, in this case interbedded siltstones and shales, plays on joint distribution. Early cross-fold joints within the formation were restricted to the siltstones (Engelder, 1985). One explanation is that flute casts and large fossil fragments are more common within the siltstone. However, early jointing within the siltstone may also be explained by the tendency of siltstones to have a lower ν than shales (Figure 5). At a $P_p = 69$ MPa a siltstone with $\nu = 0.17$ will crack whereas a shale with a $\nu = 0.25$ will remain uncracked.

5 CONCLUSIONS

Application of the principles of linear elastic fracture mechanics to the problem of joint initiation shows that in situ NHF is theoretically possible. Analysis of cross-fold joints within the Ithaca siltstone suggests that initiation took place under conditions found in a tectonically relaxed basin where the pore pressure was well above hydrostatic ($\lambda \approx 0.85$). The poroelastic effect through the Poisson's ratio of the Ithaca siltstone would have had a major effect on the exact pore pressure conditions for crack propagation. Once the cross-fold joints had propagated to lengths in excess of 1 m, the internal fracture pressure necessary for crack propagation was considerably less ($\lambda \approx 0.60$).

ACKNOWLEDGEMENTS This work was supported by Gas Research Institute contract No. 5088-260-1746. A portion of this paper was clarified as a consequence of a discussion with Chuch Mase.

REFERENCES

Anderson, R.A. Ingram, D.S. & Zanier, A.M. 1973. Determining fracture pressure gradients from well logs. Journal of Petroleum Technology 26: 1259-1268.

Bahat, D. & Engelder, T. 1984. Surface morphology on cross-fold joints of the Appalachian Plateau, New York and Pennsylvania. Tectononphysics 104: 299-313.

Beach A. 1977. Vein arrays, hydraulic fractures, and pressure solution structures in a deformed flysch sequence, S.W., England. Tectonophysics 40: 201-225.

Biot, M.A. 1941. General theory of three-dimensional consolidation. Journal of Applied Physics 12: 155-164.

Broek, D. 1987. Elementary engineering fracture mechanics: Martinus Nijhoff, Dordrecht, The Netherlands 516 p.

Engelder, T. 1985. Loading paths to joint propagation during a tectonic cycle: An example from the Appalachian Plateau, U.S.A. Journal of Structural Geology 7: 459-476.

Engelder, T. & Geiser, P.A. 1980. On the use of regional joint sets as trajectories of paleostress fields during the development of the Appalachian Plateau, New York. Journal of Geophysical Research 85: 6319-6341.

Engelder, T. Geiser, P. & Bahat, D. 1987. Alleghanian deformation within shales and siltstones of the Upper Devonian Appalachian Basin, Finger Lakes District, New York, in Roy, D., ed., Geological Society of America Centennial Field Guide - Northeastern Section 113 -118.

Engelder, T. & Oertel, G. 1985. The correlation between undercompaction and tectonic jointing within the Devonian Catskill Delta: Geology 13: 863-866.

Evans, K. Oertel, G. & Engelder, T. 1989. Appalachian Stress Study 2: Analysis of Devonian shale core: Some implications for the nature of contemporary stress variations and Alleghanian deformation in Devonian rocks: Journal of Geophysical Research 94: 7155-7170.

Fyfe, W.S. Price, N.J. & Thompson, A.B. 1978. Fluids in the Earth's Crust. Elsevier, New York, 383 p.

Geertsma, J. 1957. The effect of fluid pressure decline on volumetric changes of porous rock, Trans. AIME 210: 331-339.

Gretener, P.E. 1981. Pore Pressure: Fundamentals, general ramifications, and implications for sturctural geology. American Association of Petroleum Geologists Educational Course Note Series #4, 131 p.

Horii, H. & Nemat-Nasser, S. 1985. Compression-induced microcrack growth in brittle solids: axial splitting and shear failure. Journal of Geophysical Research 90: 3105 - 3125.

Lacazette, A. & Engelder, T. 1987. Reducing fluids and the origin of natural fractures in the Bald Eagle Sandstone, Pennsylvania, Geological Society of America Abstracts with Programs. 19: 737.

Lawn B.R. & Wilshaw, T.R. 1975. Fracture of Brittle Solids, Cambridge Univrsity Press, Cambridge, London, 204 p.

Narr, W. & Currie, J.B. 1982. Origin of fracture porosity - Example from Altamont field, Utah, Bulletin of American Association of Petroleum Geologists. 66: 1231-1247.

Nur, A. & Byerlee, J. D. 1971. An exact effective stress law for elastic deformation of rocks with fluids, Journal of Geophysical Research 76: 6414-6419.

Rice, J.R. & Cleary, M.P. 1976. Some basic diffusion solutions for fluid-saturated elastic porous media with compressible constituents: Reviews of Geophysics and Space Physics 14: 227-241.

Scott, P.A. 1989. Analysis of the correlation between fracture toughness and surface roughness on joints in the Ithaca siltstone, Watkins Glen, New York, M.S. University Park, Pa., 89 p.

Secor, D.T. 1965. Role of fluid pressure in jointing: American Journal of Science. 263: 633-646.

Secor, D.T. 1969. Mechanics of natural extension fracturing at depth in the earth's crust: Geological Survey of Canada Paper 68-52: 3-48.

Voight, B. & St.Pierre, B.H.P. 1974. Stress history and rock stress Advances in Rock Mechanics, Proceedings 3rd Congress ISRM II: 580-582.